Published in final edited form as:
Matrix Biol. 2011 May ; 30(4): 290–300. doi:10.1016/j.matbio.2011.04.004.

SCARLESS SKIN WOUND HEALING IN FOXN1 DEFICIENT (NUDE) MICE IS ASSOCIATED WITH DISTINCTIVE MATRIX METALLOPROTEINASE EXPRESSION

Barbara Gawronska-Kozak
Regenerative Biology Laboratory, Pennington Biomedical Research Center, Baton Rouge, LA, USA. Institute of Animal Reproduction and Food Research of Polish Academy of Sciences, Olsztyn, Poland

Abstract

Similar to mammalian fetuses FOXN1 deficient (nude) mice are able to restore the structure and integrity of injured skin in a scarless healing process by mechanisms independent of the genetic background. Matrix metalloproteinases (MMPs) are required for regular skin wound healing and the distinctive pattern of their expression has been implicated to promote scarless healing. In this study, we analyzed the temporal and spatial expression patterns of these molecules during the incisional skin wounds in adult nude mice. Macroscopic and histological analyses of skin wounds revealed an accelerated wound healing process, minimal granulation tissue formation and markedly diminished scarring in nude mice. Quantitative RT-PCR (*Mmp-2*,*-3*,*-8*,*-9*,*-10*,*-12*,*-13*,*-14* and *Timp-1*, *-2*, *-3*), Western blots (MMP-13) and gelatin zymography (MMP-9) revealed that MMP-9 and MMP-13 showed a unique, bimodal pattern of up-regulation during the early and late phases of wound healing in nude mice. Immunohistochemically MMP-9 and MMP-13 were generally detected in epidermis during the early phase and in dermis during the late (remodeling) phase. Consistent with these in vivo observations, dermal fibroblasts cultured from nude mice expressed higher levels of type I and III collagen, MMP-9 and MMP-13 mRNA levels and higher MMP enzyme activity than wild type controls. Collectively, these finding suggest that the bimodal pattern of MMP-9 and MMP-13 expression during skin repair process in nude mice could be a major component of their ability for scarless healing.

Keywords

matrix metalloproteinases; wound healing; regeneration; FOXN1; nude mice

1. Introduction

Skin injury in adult mammals initiates a series of coordinated events involving inflammation, reepithelialization, angiogenesis, granulation tissues formation and matrix

Corresponding author: Barbara Gawronska-Kozak, Institute of Animal Reproduction and Food Research of Polish Academy of Sciences, Olsztyn, Poland, ul. Tuwima 10, 10-747 Olsztyn, Poland, Telephone (4889) 5234621, Fax (4889) 5240124, b.kozak@pan.olsztyn.pl.

deposition, steps in the healing process that generate scar tissue. In contrast to mammals, invertebrates (e.g. planarians) and some vertebrate species (e.g., zebrafish and urodele amphibians) respond to injury by a regenerative scar-free process that completely restores anatomical and physiological characteristics of post-injured tissues (Bryant et al., 2002; Gurtner et al., 2008). However, even certain mammalian tissues have shown the capacity for regeneration including digit tips in children and mouse (Han et al., 2008), ears in rabbit and MRL mice (Clark et al., 1998), embryonic and fetal skin (Colwell et al., 2005; Ferguson and O'Kane, 2004) and ear and skin of FOXN1 deficient nude mice (Gawronska-Kozak, 2004; Gawronska-Kozak et al., 2006; Manuel and Gawronska-Kozak, 2006). Whereas skin wounds in adult mammals heal with scar, in fetuses integrity of skin after injury is restored through a process resembling regeneration (Colwell et al., 2005; Ferguson and O'Kane, 2004; Martin, 1997). Intriguingly, scarless skin healing, similar to that observed in mammalian fetuses, also occurs in aged animals and humans (Ashcroft et al., 1997a; Ashcroft et al., 1997b).

Although the mechanisms that underlie scarless skin repair in fetuses are incompletely understood (Gurtner et al., 2008), this phenomenon has been linked to the low or absent inflammatory response, high levels of hyaluronic acid, the dynamics of collagen deposition and altered expression of matrix metalloproteinases (MMPs) and their tissue inhibitors (TIMPs) (Colwell et al., 2005; Ferguson and O'Kane, 2004; Longaker et al., 1990; Redd et al., 2004).

Matrix metalloproteinases constitute a family of zinc endopeptidases that are capable of degrading most of the structural components of the extracellular matrix (ECM) (Gill and Parks, 2008; Page-McCaw et al., 2007; Parks, 1999). Because of the broad substrate spectrum of MMPs action, they participate in many biological processes such as development, morphogenesis, regeneration, and wound healing (Page-McCaw et al., 2007). Cutaneous wound repair is comprised of several processes requiring the action of proteinases: invasion of inflammatory cells, migration of keratinocytes and fibroblasts, angiogenesis, wound contraction and finally remodeling of the scar tissues (Clark, 1996; Gill and Parks, 2008; Martin, 1997). Distinct patterns of MMPs and TIMPs expression have been observed during different phases of regular skin wound repair (Gill and Parks, 2008; Madlener et al., 1998; Soo et al., 2000; Vaalamo et al., 1999). The expression patterns of collagenases (MMP-11, -8,-13), gelatinases (MMP-2, -9), stromelysins (MMP-3, -10), macrophage metalloelastases (MMP-12), membrane-type MMPs (MMP-14) and TIMP-1,-2,-3 have been shown to be distributed among cells participating in skin repair (Gill and Parks, 2008; Madlener et al., 1998; Parks, 1999; Soo et al., 2000). Because the activity of MMPs affects many diverse processes, their action is stringently regulated at the levels of transcription, post-transcriptional modulation, protein secretion, extracellular activation upon their release from latency and finally through the action of TIMPs, the natural tissue inhibitors of MMPs (Page-McCaw et al., 2007; Steffensen et al., 2001). Although MMPs are indispensable for regular repair, it has been proposed that the deregulation of the fine balance between MMPs and TIMPs during the wound healing process leads to pathological situations such as the inability of chronic wounds to heal (Wysocki et al., 1993) or keloid scar formation (Fujiwara et al., 2005). However, inappropriate expression or overexpression does not always lead to impaired healing. In specific circumstances, it might be an important element for perfect healing (regeneration) as observed during regeneration in amphibians (Vinarsky et al., 2005; Yang et al., 1999). Yang et al., and Vinarsky et al., showed that MMP-9 displays a distinctive bimodal pattern of activity during early and late stages of limb regeneration in amphibians (Vinarsky et al., 2005; Yang et al., 1999). Moreover, elevated levels of MMP expression have been also detected during skin scar-free healing in mammalian fetuses (Dang et al., 2003b) and during

scar-less skin healing in aged animals and humans (Ashcroft et al., 1997a; Ashcroft et al., 1997b).

Our laboratory has shown that FOXN1 deficient (nude) mice exhibit a scarless wound healing process of skin that resembles regeneration (Gawronska-Kozak et al., 2006; Manuel and Gawronska-Kozak, 2006). Since the nude phenotype, resulting from inactivation of the transcription factor FOXN1, is characterized by the lack of visible hair and immunodeficiency (the absence of thymus and T-cells), we previously tested the hypothesis that skin regeneration in nude mice was due to T-cell deficiency and/or lack of thymus. The experiment, performed on several murine models on the C57BL/6J (B6) background, revealed that scarless skin healing occurred exclusively in nude mice and was not a consequence of immunodeficiency. The post-injured skin of nude mice was characterized by markedly diminished scarring, low levels of collagen content, high levels of hyaluronic acid, low levels of pro-scarring cytokines and showed substantial differences in MMP-9 expression in skin between FOXN1 deficient (nude) and wild type mice (Gawronska-Kozak et al., 2006; Manuel and Gawronska-Kozak, 2006). Although the data did not exclude the possibility that an inflammatory response is involved in the outcome of skin wound healing process, they strongly showed that the lack of thymus and/or T-cells were not sufficient to support scarless healing. Since skin wound healing in general requires the coordinated action of multiple MMPs/TIMPs and the distinctive pattern of their expression has been implicated in scarless healing in mammalian fetuses, in this study we have (i) characterized the expression of MMPs/TIMPs and collagen in the skin tissues of nude and wild type mice during wound healing *in vivo* and (ii) determined whether these characteristics are retained in dermal fibroblasts *in vitro*.

2. Results

Our previous results demonstrated that FOXN1 deficient (nude) mice (B6.Cg-*Foxn1*^{nu}), unlike other immunodeficient, athymic or wild type mice (all B6 genetic background), show an ability to heal skin incisions with markedly diminished scarring (Gawronska-Kozak et al., 2006). This ability was accompanied by high levels of MMP-9 expression at Day 24 after wounding (Manuel and Gawronska-Kozak, 2006). In the present study we first established that scarless healing occurs not only in nude on B6 background but also in nude on mix genetic background. We analyzed skin wound healing process and MMPs/TIMPs expression in nude (Hsd: Athymic Nude-*Foxn1*^{nu}) mice. As a non-mutant control we used the closely related BALB/c strain of mice. Macroscopic evaluation of post-injured area showed that skin incisions caused minimal bleeding and rapid skin closure in FOXN1 deficient, but not in wild type mice. Figure 1 depicts post-wounded skin area at Day 7 after injury in wild type (A) and nude (B) mice. Whereas FOXN1 deficient mice displayed a fine narrow line that marks the incision site (Fig. 1B), wild type mice acquired a prominent scab at the injury site (Fig. 1A). These observations based on Hsd: Athymic Nude-*Foxn1*^{nu} mice are in agreement with our previous results performed on B6.Cg-*Foxn1*^{nu} (Gawronska-Kozak et al., 2006), indicating that scarless healing of skin in FOXN1 deficient mice is independent of their genetic background.

2.1. Collagen accumulation

Since the family of collagens is a major component of the wound extracellular matrix (Clark, 1996) and the major substrate for MMPs action (Steffensen et al., 2001), we analyzed its content by measuring hydroxyproline levels in uninjured and post-injured skin samples. Figure 2 shows that differences in collagen content were already present in uninjured skin tissues. Collagen levels in uninjured skin tissues measured as hydroxyproline content were much lower in nude than in control mice ($p<0.001$; Fig. 2 Day 0). After injury, the collagen content immediately declined in both nude and wild-type mice. The recovery of

collagen in nude mice begins as early as Day 3, remains high between Days 5 and 7 and then gradually decreases. At Day 21 collagen content stabilized at the levels observed in uninjured skin tissues and remained unchanged until the end of the experiment. On the other hand, post-injured skin tissues of control animals showed the lowest collagen content at Day 5, comparable to that observed in nude mice at Day 3 (Fig. 2). A slow increase in hydroxyproline levels in postinjured skin tissues was observed between Days 5 and 36; however, the collagen content never reached levels observed in wild type uninjured skin tissues (Fig. 2). Although statistical significant differences in collagen levels were observed between nude and wild type mice during the early days following injury, the eventual recovery to similar collagen levels by 21 days suggests that the differences in collagen content per se do not explain the differences in wound healing.

2.2. MMPs and TIMPs mRNA expression in skin tissues

To explore the differences in MMPs/TIMPs gene expression between FOXN1 deficient and wild type mice, we first determined mRNA levels (nude; n=7–9 and wild type; n=7–9) in uninjured skin. As shown in Table 1 the expression levels of most MMPs (but not MMP-2) tended to be higher in the skin of FOXN1 deficient mice; however, statistical significant differences were only observed for *Mmp-12* and *Mmp-13* (Table 1). Differences in the mRNA content of TIMPs in skin were not statistically significant between nude and wild type mice (Table 1).

Next, we compare MMPs and TIMPs expression levels in post-injured skin tissues from FOXN1 deficient and wild type mice during the time course of wound healing process (Fig. 3). Skin injury at post-wounded Days 1–3 evoked a rapid up-regulation of *Mmp-9, Mmp-13, Mmp-3, Mmp-8, Mmp-10* and *Timp-1* mRNA levels in both mouse strains. However, the magnitude of up-regulation was much lower in nude mice. The increase in *Mmp-9* was only 30% of that observed for control mice and for *Mmp-8* and *Timp-1* it was 25% and 50% respectively (Fig. 3). This initial up-regulation of *Mmps* mRNA expression was followed by a gradual decrease between days 5–36 in nude and wild type animals. Nude mice showed levels of *Mmp-3, Mmp-13, Mmp-8, Mmp-9, Mmp-10* and *Timp-1* expression at post-injured day 7 comparable to those observed before injury. However, the most striking and consistent differences in MMPs expression were detected between Days 21–36 of wound healing. FOXN1 deficient mice showed a second wave of elevated *Mmp-9, Mmp-13* and to some extend *Mmp-10* and *Timp-1* mRNA expression that did not occur in wild type tissues. In contrast, post injured skin tissues from control mice displayed low, unchanged mRNA expression until the end of experiment at Day 36.

The skin injury caused changes in mRNA expression of other *Mmps* as well. *Mmp-2, Mmp-12, Mmp-14* and *Timp-2* were up-regulated in wild type mice after injury and sustained high levels until Day 14. Interestingly, at Day 14, the expression of *Mmp-2, Mmp-3, Mmp-12*, and *Timp-1* mRNA in wild mice was higher than before injury and significantly higher than in nude mice (*Mmp-2* $p<0.01$; *Mmp-3* $p<0.001$; *Mmp-12* $p<0.001$; *Timp-1* $p<0.001$; Fig. 3). Comparable samples from nude mice showed modest upregulation of *Mmp-2*, *Mmp-3* and *Mmp-12* at Day 1–3 that decreased to the levels observed in un-injured skin between Days 5–7 (Fig. 3). *Timp-3* mRNA levels were significantly down-regulated between days 1–3, followed by a gradual increase until Day 36, with no differences in expression between nude and wild-type mice (Fig. 3).

2.3. MMP-9 and MMP-13 protein expression/activity in post-injured skin tissues

Since *Mmp-9* and *Mmp-13* mRNA levels were significantly different between nude and wild type mice at 36 days process, we assessed changes in MMP-9 and MMP-13 protein levels by gelatin zymography (MMP-9; Fig. 4A – D) and Western blot (MMP-13; Fig. 4E – G)

assays. Zymography of MMP-9 enzymatic activity showed two dominant white bands on Comassie Blue-stained zymogram gels corresponding to pro-MMP-9 (97kDa) and active MMP-9 (87kDa) forms (Fig. 4A and C). Zymograms of individual skin samples collected from nude and wild type mice during the course of wound healing revealed a pattern of MMP-9 protein expression similar to mRNA. Injury caused rapid elevation of pro-MMP-9 expression between post-injured Days 1 and 5 (Fig. 4A, B and D) in both nude and control mice, although the induction was significantly attenuated in nude mice ($p<0.001$) compared to wild type mice (Fig. 4B). From Day 5 to 21 a gradual decrease in pro and active form of MMP-9 protein was observed in both nude and wild type mice (Fig. 4B and D). Whereas MMP-9 protein in control mice became undetectable from Day 14 until the end of experiment (Day 36), in nude mice MMP-9 protein levels were induced between Days 21 and 36 (active-MMP-9 Fig. 4D $p<0.05$). This pattern of protein expression is in agreement with qRT-PCR data for *Mmp-9* mRNA expression (compare Fig. 3). Although the expression level at Day 36 was variable among individual nude samples, the MMP-9 activity was virtually undetectable in wild-type mice (Fig. 4C).

Western blots demonstrated a pattern of MMP-13 protein expression that was comparable to the MMP-9 activity described in the preceding paragraph (Fig. 4E–G). Generally, MMP-13 protein bands were much stronger in skin samples from nude mice at each day after injury (Fig. 4E). However, the most striking differences were observed at Day 36 (Fig. 4E–G) where MMP-13 levels in individual skin samples from nude (n=6) were consistently elevated while the protein band for MMP-13 in all control mice (n=6) was essentially undetectable (Fig. 4G). Densitometric analysis revealed statistical significant differences in MMP-13 protein expression between nude and wild type mice at day 36 (5 fold increase in nude skin tissues; $p<0.001$; Fig. 4F).

2.4. Histological and immunohistological analysis of post-wounded skin tissues

Masson's trichrome stained histological sections of unwounded skin samples showed more collagen content (blue staining) in wild type than nude skin that is in agreement with the data on skin hydroxyproline content at Day 0 (compare Fig. 5A, B, and Fig 2). Histological examination of postinjured skin tissues revealed striking differences in wound healing between nude and wild type mice (Figure 5). In particular, the timing of occurrence of wound healing stages varied dramatically between nude and wild type mice (compare Fig. 5E and 5F, 5G and 5H).

Microscopical examination of Masson's trichrome stained sections confirmed our visual observations that the healing process of incisional wounds in nude mice is accelerated and scarring is markedly diminished (Fig. 5). Complete wound site closure in nude mice was observed between Day 1 and 3 (Fig. 5C and 5E) whereas wild type mice required an additional 2 days to close their wounds between Days 3 and 5 (Fig. 5F and 5H). Scab formation was detected in all wild type mice (Fig. 5H), but almost never in nude mice. At Day 3, granulation tissues were present in the post-injured area in nude mice (Fig. 5E), whereas a similar structure did not form in wild type mice until Day 5–7 (Fig. 5H). The presence of granulation tissues in nude mice (Day 3–5) and wild type mice (Day 5–7) correlate with intense collagen synthesis during the same time period (compare Fig. 5E, H, and Fig. 2). At Day 7 after injury, wound areas of nude mice are smaller and narrower than corresponding regions in wild type mice (compare Fig. 5G and 5H). Additionally, epidermis in post-injured tissues at Day 7 in nude mice forms a thin layer similar to the uninjured. On the other hand wild type mice showed a thick, multilayered structure easily differentiated from un-injured skin (compare Fig. 5G and H). At Days 14, 21 (not shown) and 36 post-injured skin tissues were difficult to distinguish from surrounding un-injured tissues in nude mice (Fig. 5I and 5K). Masson's trichrome blue-stained collagen fibers appeared as a very fine line among subcutaneous fat tissues on Day 14 (Fig. 5I - arrows) that were undetectable

at day 36 (Fig. 5K – arrow). In contrast, wild type mice display well-defined, disorganized collagen bundles penetrating the dermis, subcutaneous fat pads and underlying muscle (Fig. 5J and 5L). The width of the scar tissue was measured. At Day 36 mean scar width for wild type mice was 52.6 μm (Fig. 5L) whereas wounds of nude mice were hardly detectable, with a mean scar width of 4.5 μm (Fig. 5K: $p<0.001$).

To evaluate MMP-9 and MMP-13 expression *in situ*, alternative histological sections were stained by Masson's trichrome for collagen and for MMPs by immunohistochemistry approach (MMP-9 Fig. 6A–D; MMP-13 Fig. 6E–J). At postwounded Day 3 MMP-9 expression was present in epidermis and granulation tissues (fibroblasts-like cells and inflammatory cells) in nude skin tissues (Fig. 6A). Corresponding sections from control mice showed MMP-9 expression in epidermis and in inflammatory cells localized within subcutaneous fat layer (Fig. 6B). However, the most prominent differences in MMP-9 expression between nude and wild type mice were detected on day 21 (data not shown) and Day 36 (Fig. 6C and 6D). Whereas epidermis was positive for MMP-9 expression in both nude and control animals, MMP-9 positive fibroblast-like cells were uniformly spread through post-wounded dermal tissues in nude, but not wild type mice.

Strong MMP-13 immunoreactivity at post-injured Day 1–3 was detected in the epidermal layer in proximity to the wounded area and in the dermal part of skin, especially at the epidermal/dermal junction in both nude (Fig. 6E) and control mice (Fig. 6F). Additionally, very prominent MMP-13 staining in nude mice was localized to granulation tissues at Day 3 (Fig. 6E). Comparable sections from control mice were observed on Day 7; however, MMP-13 staining was less intense (Fig. 6H). Immunohistochemical data of MMP-13 expression correlates with Western blot analysis. Intense MMP-13 staining at Day 3 in nude mice (Fig. 6E) supports high levels of MMP-13 protein expression (compare Fig. 4F). Following injury on days 7–36, epidermal staining for MMP-13 disappeared in nude and wild type mice (Fig. 6G–J). However, dermal part of the skin in nude mice displayed an abundance of MMP-13 expression (Fig. 6G and 6I) whereas wild type mice showed only a few dermal cells positive for MMP-13 in proximity to the epidermal-dermal junction (Fig. 6H and 6J).

Summarizing the immunohistological data we emphasize that expression of both MMP-9 and MMP-13 was prominent in the first phase of wound healing in both nude and wild type mice in epidermis of the skin. However, the staining intensity in epidermis was reduced for MMP-9 and disappeared for MMP-13 during the course of wound healing in both nude and wild type mice. In contrast, a strong positive expression for MMP-9 and MMP-13 was acquired in the dermis of skin (fibroblast-like cells) during the remodeling phase of wound healing that is unique for nude mice.

2.5. Collagen mRNA expression and MMP-9, MMP-13 expression/activity in dermal fibroblasts from nude and wild type mice

Following injury, fibroblasts play a central role in the healing response through the synthesis and deposition of components of new tissues (ie. collagen) and through remodeling post-injured skin tissues, i.e. via secretion of MMPs (Clark, 1996). Intrinsic differences in fibroblasts have been proposed to be responsible for scarless skin healing in mammalian fetuses (Lorenz et al., 1995), gingival wounds (Ravanti et al., 1999) and in regenerating limbs in amphibians (Bryant et al., 2002). Since our *in vivo* data showed accelerated collagen deposition (compare Fig. 2 and Fig. 5) and differences in MMPs expression in post-wounded nude skin tissues, we asked whether these phenotypic differences are retained by fibroblasts derived from nude and wild type mice. To address this question we performed *in vitro* studies in which we analyzed collagen I and collagen III gene expression and MMP-13 and MMP-9 production/activity in nude and B6 dermal fibroblasts. Figure 7

illustrates the results of our study. Quantitative RT-PCR analysis showed that nude dermal fibroblasts cultured under the same conditions (seeding density, collagen IV coated dishes, passage=1) as B6 wild-type cells displayed significantly higher mRNA expression for type I (Fig. 7A) and type III (Fig. 7B) collagen. Similarly, RNA levels for MMP-9 and MMP-13 were 5-fold and 6.5-fold (respectively) higher in nude dermal fibroblasts (Fig. 7C). To examine MMPs activity we performed in situ zymography with quenched fluorogenic (FITC) DQ-gelatin and DQ-collagen IV (Fig. 7D–H). The principle of the method posits that cell-released active metalloproteinases cleave dye-quenched (DQ)-gelatin and DQ-collagen IV to produce fluorescent peptides that can be visualized. The method allows for rapid and highly sensitive assessment of proteolytic activity. In 24-hour incubated cells we detected high degradation of gelatin (Fig. 7D) and collagen IV (Fig. 7G) by nude dermal fibroblasts that was entirely absent (Fig. 7E) or at very low levels (Fig. 7H) in B6. Furthermore, gelatinolytic activity was abrogated/blocked in the presence of metalloproteinases inhibitor GM6001 (Fig. 7F), suggesting the activity is specific for MMP. Those observations were further confirmed by standard zymography (Fig. 7I). Whereas MMP-2 protein expression was detected in both types of dermal fibroblasts, MMP-9 was identified in nude but not wild type.

Summarizing results, the *in vivo* data correspond with *in vitro* results. Collagen content in post-injured tissues (Fig. 2) and matched trichrome-stained histological sections (Fig. 5A and B) showed lower collagen content in un-injured nude skin. After injury nude mice showed very rapid replacement of collagen in post-injured area (Fig. 2 and Fig. 5). Accelerated granulation tissue formation/decrease has been observed in nude mice (compare Fig. 5E–G and Fig. 5H–J). The major decrease in the area of the granulation tissues in nude mice, achieved between Days 3–7, suggests a shift in the balance of collagen synthesis and degradation. This suggestion is supported by high levels of MMP-9 and MMP-13 expression in nude granulation tissues (Fig. 6A (dermal fibroblasts), 4E–F and 6E) and the ability of nude dermal fibroblasts to synthesize higher than wild type levels of collagens and MMP-9, -13 (Fig. 7). The last phase of wound healing in nude mice is accompanied by a second weave of MMP-9 and MMP-13 up-regulation (Fig. 3, Fig. 4, Fig. 6C and 6I) that corresponds with markedly diminished scarring (compare Fig. 5K and 5L).

3. Discussion

In this study we have shown that mice carrying a mutation that inactivates the transcriptional factor FOXN1 can heal skin injuries with a reduction in scarring that resembles scarless healing. This effect of nude on wound healing is independent of the genetic background. Our data demonstrated that scarless skin healing in nude mice is accompanied by elevated levels of MMP-9 and MMP-13 expression, first during the inflammatory phase and then during remodeling phase of wound skin healing. These patterns of MMPs expression resemble those that occur during limb regeneration in amphibians.

The robust changes in expression of MMPs/TIMPs are a reproducible feature of regular skin wound healing processes (Hattori et al., 2009; Kyriakides et al., 2009; Madlener et al., 1998; Parks, 1999; Soo et al., 2000; Vaalamo et al., 1999). Rapid upregulation of MMP-1, -2, -3, -8, -9, -10, -12, -13, -14 and TIMP-1, -2 occurred during first phase of wound healing and then gradually decreased as the healing process progressed (Madlener et al., 1998; Soo et al., 2000). Similar expression patterns occurred during the course of wound healing in control mice in our study (see Fig. 3 and 4). Opposite to controls, the nude mice showed a distinctive, bimodal pattern of MMP-9 and MMP-13 expression during the early (Days 1–5) and late (Days 21–36) phase of wound healing. We hypothesize that the bimodal pattern of MMPs expression during skin wound healing is associated with nude's ability for scarless healing. A similar association for MMPs expression and tissue remodeling was observed

during limb regeneration in amphibians (Vinarsky et al., 2005; Yang et al., 1999). These authors suggest that the bimodal pattern of MMP-9 expression might prevent scar formation, while promoting the deposition of an ECM conducive to regeneration. Similarly, scarless healing in mammalian fetuses has been attributable to the unusual balance between MMP and TIMP expression that is shifted towards higher expression of MMPs and lower levels of TIMPs (Dang et al., 2003b). The up-regulation of MMP-2 and MMP-9 expression and activity until post-wounded day 21 in elderly human and animal models has been associated with their ability to heal with a better quality of scarring possibly due to regeneration of dermal architecture (Ashcroft et al., 1997b; Ashcroft et al., 2002). Interestingly, a bimodal pattern of MMP-13 expression was also observed during superior healing after free-electron laser surgery in transgenic mouse strain with the MMP-13 promoter driving luciferase expression (Wu et al., 2003).

To identify the function of MMP-9 and MMP-13 in the wound healing process genetics knockout experiments were performed. Studies by Hartenstein et al., showed that MMP-13 KO mice were no different in wound closure efficiency than wild type mice (Hartenstein et al., 2006). On the other hand, Kyriakides et al. and Hattori et al. analyzing the wound healing process in MMP-9KO, MMP-13KO and MMP9/MMP-13/double knockout mice (Hattori et al., 2009; Kyriakides et al., 2009) showed that all MMPKO mice displayed a delay in wound closure with the longest attenuation being observed at Day 10 for double KO mice (Hattori et al., 2009). The delay was reversed by topical treatment of wounds with recombinant MMP-9 and MMP-13. Although these studies with knockout models showed that MMPs are necessary for the wound healing process, the precise role of MMPs in healing/scar formation has not been determined.

Since MMPs are produced by many cell types in the skin, their role depends on the emergence of relevant cell types during the healing process. It is well established that epidermal cells are the source of MMP-9 and MMP-13 expression during first stage of healing (Clark, 1996; Hattori et al., 2009; Legrand et al., 1999; Madlener et al., 1998; Wu et al., 2003). The present immunohistochemical analysis showed MMP-9 and MMP-13 expression in the epidermal cells at the leading edge of the wound in both nude and control mice during first postwounded days (see Fig. 6). The MMP-9 and MMP-13 expression in migrating epithelial sheet in healing wounds has been postulated to promote epithelial resurfacing by stimulating cell migration (Hattori et al., 2009; Legrand et al., 1999) and coordinating epithelial regeneration (Mohan et al., 2002). Inflammatory cells (T-cells, PMN, neutrophils, eosinophils and macrophages) are the next source of MMP-9 expression in injured skin (Barrick et al., 1999; Clark, 1996; Hattori et al., 2009; Madlener et al., 1998). This MMP-9 activity is believed to be involved in inflammatory cell migration and recruitment to the wound site (Owen et al., 2003). Interestingly, whereas control mice in our study showed a surge of inflammatory-connected MMPs as MMP-9 (by eosinophils), MMP-8 (by neutrophils) and MMP-12 (by macrophages) (Park and Kim, 1999), the increase in nude mice expression was attenuated (see Fig. 3). These data, together with T-cell deficiency in nude mice and similar levels of macrophage content in post-wounded skin tissues between nude and wild type mice (Manuel and Gawronska-Kozak, 2006), are consistent with observations that wounds to the skin of mammalian fetuses and gingival tissue showed reduced inflammation during the healing process, a condition that has been linked to scarless healing (Colwell et al., 2005; Redd et al., 2004; Szpaderska et al., 2003).

The expression of MMP-9 and MMP-13 by dermal fibroblasts and therefore their participation in late phase of wound healing is controversial in the literature. Although most of the studies indicate that dermal fibroblasts do not express MMP-9, it has been shown that TGF β1 and tumor necrosis factor α (TNFα) stimulate MMP-9 expression in human dermal fibroblasts (Han et al., 2001; Kobayashi et al., 2003). Moreover, Peled et al. showed

differences in MMP-2 and MMP-9 expression between fetal fibroblasts from scar-free and scar-forming stages of gestation (Peled et al., 2002). Similarly, abundant MMP-13 expression was detected in fibroblasts from gingival wounds and fetal skin wounds which heal with minimal scarring (Ravanti et al., 1999; Ravanti et al., 2001) suggesting a role for MMP-13 in scarless repair (Toriseva and Kahari, 2009). Intriguingly, higher levels of MMPs expression during scar-free healing accompanied high levels of TGFβ3 expression implicating the latter as a key regulator of the scar-free phenotype in embryonic healing (Occleston et al., 2008a; Occleston et al., 2008b; Ravanti et al., 2001). In the present studies we detected substantial differences in MMP-9, MMP-13 and collagen expression between nude and wild type dermal fibroblasts. Our data indicate that nude dermal fibroblasts are capable of rapid and abundant expression of collagen I and collagen III. Interestingly, high levels of collagen III in post-wounded fetal skin tissues are considered as a hallmark of scar-free healing (Dang et al., 2003a; Longaker et al., 1990). Rapid and high expression of collagen and simultaneous high levels of MMP-9 and MMP-13 expression by nude dermal fibroblasts can at least partially explain rapid collagen turnover (production vs degradation) and different kinetics of wound reorganization. By Day 21 collagen content in nude mice was similar to that observed in uninjured samples, indicating an equilibrium in factors influencing collagen synthesis, degradation and remodeling. Corresponding skin tissues from control animals showed longer recovery and significantly lower levels of collagen that did not regain levels observed before injury (see Fig. 2). Similar to our observations, scarless healing in fetal skin wounds was attributed to rapid collagen remodeling (Longaker et al., 1990; Toriseva et al., 2007).

Our previous results and the present findings consistently suggest that MMP-9 and MMP-13 activity may facilitate skin wound healing with minimal scarring in nude mice (Manuel and Gawronska-Kozak, 2006). However, the key question is how they fulfill their role. We speculate that MMP-9 and MMP-13 released by fibroblasts facilitates the migration of these cells and participates in collagen remodeling during the last phase of healing.

In conclusion, the results of the present study showed that FOXN1 deficient (nude) mice displayed accelerated wound healing process, minimal granulation tissue formation and markedly diminished scarring. The nude skin wound healing process is characterized by a bimodal pattern of MMP-9 and MMP-13 expression that accompanies rapid collagen turnover. We hypothesize that the secondary induction of MMP-9 and MMP-13 expression observed in the dermal part of skin during the remodeling phase of wound healing is necessary to initiate the cascade of events that contribute to scarless healing in nude mice.

4. Experimental Procedures

4.1. Animals and Wound Model

The present study was performed on 6-week old Hsd: Athymic Nude-Foxn1nu (n= 65) and BALB/c (n=65) female mice obtained from Harlan Sprague-Dawley (Indianapolis, IN). The day before the wounding procedure the hair of wild type mice was shaved in the dorsal area. At the time of wounding, animals were anesthetized by isoflurane anesthetics. Mice were given a 3–4 cm full-thickness dorsal wound that was closed with three stainless steel wound clips. The staples were removed 5 days after wounding. The surgical procedures for all animals were performed in sterile conditions under a laminar hood. Animals were sacrificed on Day 1, 3, 5, 7, 14, 21, and 36 (n=7–9 per group) after wounding and skin samples (8 mm diameter) were collected from the area between wound clips (marked with arrows) (Fig. 1). Two 8 mm diameter skin biopsy punches from each animal were frozen in liquid nitrogen for protein and RNA isolation. Additionally, the third biopsy punch was frozen in liquid nitrogen for hydroxyproline assay or fixed in formalin for histological analysis.

The experimental animal procedures performed in these studies have been approved by the Institutional Animal Care and Use Committee at the Pennington Biomedical Research Center.

4.2. RNA isolation and quantitative RT-PCR

Total RNA was extracted using Trizol (Invitrogen, Carlsbad, CA) and column-purified with RNeasy and RNase-Free DNase kits (Qiagen, Valencia, CA). cDNA synthesis was performed with 500 ng of total RNA using the High Capacity cDNA Archive Kit (Applied Biosystems, Foster City, CA). Endogenous mRNA levels for: MMP-2, MMP-3, MMP-8, MMP-9, MMP-10, MMP-12, MMP-13, MMP-14, TIMP-1, TIMP-2, TIMP-3, α1 chain of type I collagen (col1a1), α2 chain of type I collagen (col1a2), α1 chain of type III collagen (col3a1) and the housekeeping genes: cyclophilin B, hypoxanthine phosphoribosyltransferase 1 (HPRT1) and glyceraldehyde-3-phosphate dehydrogenase (GAPDH) were measured with Applied Biosystems Taqman® Gene Expression Assays (Applied Biosystems, Foster City, CA). Reactions were performed in MicroAmp Optic 384-well Reaction Plates (Applied Biosystems) using the ABI Prism 7900 Sequence Detection System (Perkin Elmer, Boston, MA) under the following incubation conditions: 2 min at 48°C, 10 min at 95°C, 40 cycles of 15 s at 95°C and 1 min at 60°C. Each run included a standard curve with aliquots from a RNA pool isolated from skin tissues, a non-template control, and minus reverse transcriptase control that were analyzed in duplicate. Expression levels for each gene estimated from the standard curve were normalized to cyclophilin B (in vivo study), GAPDH or HPRT1 (in vitro study) and multiplied by 10.

4.3. Protein isolation and Western blot analysis

Frozen samples from 8 mm skin punches were powdered using a pre-chilled mortar and pestle, then homogenized in 500 μl of RIPA buffer containing proteinase inhibitor cocktail (Sigma). Protein concentrations of lysates were determined by modified Lowry protein assay 28 and 20 ug of protein were separated on 12 % SDS-polyacrylamide gels. Proteins were transferred onto polyvinylidene difluoride membranes (Millipore) and incubated with monoclonal antibodies against MMP-13 (Chemicon International, Inc.). Bands were visualized using the Odyssey imaging system (LI-COR Bioscience) with fluorescent (IRDye800TM or Cy5.5) labeled secondary antibodies according to manufacturer's protocol. Membranes were re-probed using anti-GAPDH antibody (Abcam Inc.).

4.4. Zymographic analysis

Gelatinolytic activity was determined by zymography using gelatin-containing gels following the protocol published by Chemicon International, Inc. The skin sample extracts were mixed with an equal volume of non-reducing sample buffer (0.5 M Tris-HCl, pH 6.8, SDS 10%, glycerol and bromophenol blue). Ten percent polyacrylamide gels contained 1 mg/ml of gelatin (porcine A; Sigma) dispersed in 1.5 M Tris-HCl pH 8.8, 100 μl 10% SDS, 3.3 ml of 30% acrylamide mix (Bio-Rad) and 3 ml of bidistilled water. The stacking gel contained 5% acrylamide mix in 1.0 M Tris pH 6.8. Gels were polymerized by adding 100 μl of 10% ammonium persulfate (Sigma) and 4 μl of TEMED (Sigma). 20 μg of non-denatured protein samples were loaded and electrophoresis was performed in 1X Tris/glycine/SDS running buffer (Bio-Rad) at 80V for 2.5 hours. After electrophoresis, gels were incubated in zymogram renaturing buffer (Bio-Rad) with gentle agitation for 30 min to reactivate MMP activity. Gels were then incubated in zymogram developing buffer (Bio-Rad) overnight at 37 °C with mechanical stirring. Gels were stained with Coomassie Blue (Bio-Rad) for 30 min and destained with destaining solution (Bio-Rad). Clear protein lysis bands on a blue background were visualized with a UV/white light conversion screen (Bio-Rad).

4.5. Densitometric analysis

In the first step we designed a control sample that would be used in each of the zymograph and Western Blot for MMP-9 and MMP-13, respectively. Based upon qRT-PCR data, 4 samples from nude post-injured skin were selected for zymography and Western Blot at 10, 20 and 40μg protein. We chose one sample to serve as an internal quality control standard in order to normalize densitometric data from different blots. Electrophoresis followed by Western blot for nude and wild type animals for particular time points after injury was performed simultaneously using always the same sample as an internal control. A total of 16 Western blots and 16 zymographs were completed, each contained n=7–9 samples per time point. Densitometric analyses were performed using the Odyssey LI-COR imaging system.

4.6. Immunohistochemical detection of MMP-9 and MMP-13 expression

Formalin-fixed skin samples were processed, embedded in paraffin and sectioned at 5 μm. Slides were stained with Masson's trichrome for collagen presence using standard protocol. Immunohistochemical staining for the presence of MMP-9 (polyclonal MMP-9 antibodies; BD Biosciences Pharmingen) and MMP-13 (polyclonal MMP-13 antibodies; LifeSpan BioSciences) was performed on consecutive sections. Antibody binding was detected with the ABC complex (Vectastain ABC kit, Vector Laboratories, Inc., Burlingame, CA). Two types of controls were performed: (a) the primary antibody was omitted during the immunostaining procedure; (b) the primary antibody was substituted with non-specific immunoglobulin G (IgG) during the procedure. Counterstained with hematoxylin, sections were visualized with a Zeiss microscope (Axioskop 40) and photographed with a Kodak digital camera (DC290 Zoom).

4.7. Measurement of hydroxyproline

Collagen assays were performed on 8 mm diameter skin tissues that were dissected with a dermal biopsy punch to assure the accuracy in the amount of starting material for analysis. The assay was prepared as described before 8. 8 mm diameter skin punches, which had been frozen in liquid nitrogen, were homogenized in 2 ml of phosphate buffered saline and stored in 4°C overnight. The next day, 1 ml aliquots were hydrolyzed with 0.5 ml of 6N HCL for 5h at 120°C. Samples were then cooled and 20 μl of each sample was added to a 96 well plate and incubated for 20 min at room temperature with 50 μl of chloramine T solution (282 mg chloramine T, 2ml n-propanol, 2 ml distilled water and 16 ml citrate acetate buffer [5% citric acid, 7.24% sodium acetate, 3.4 % sodium hydroxide and 1.2 % glacial acetic acid]). Then 50 μl of Ehrlich's solution (2.5 g 4-(dimethyloamino) benzaldehyde, 9.3 ml n-propanol and 3.9 ml 70% perchloric acid) was added and the plate was incubated for 15 min at 65°C. The samples were cooled and the plate was read at 550 nm on a microplate reader (Benchmark Plus, Bio-Rad). Hydroxyproline concentrations from 0 – 10 μg/ml were used to construct a standard curve.

4.8. Isolation and culture of dermal fibroblasts

Skin tissues were collected from Hsd: Athymic Nude-Foxn1nu and B6 mice, minced and digested with collagenase class I (2mg/ml; Worthington Biochemical Corp., Freehold, NJ) in a shaking water bath at 37°C for 1hour. Dissociated dermal fibroblasts were filtered through a 100μm cell strainer (Becton Dickinson Labware, NJ) and centrifuged at 360 × g for 5 min. Pelleted cells were resuspended for 1 min in red blood cell lysing buffer (Sigma Co. St. Louis, MO) to remove erythrocyte contamination and were centrifuged at 360 × g for 5 min. Cells were plated in 100 mm Petri dishes (p=0) in Dulbecco's Modified Eagle Medium (DMEM/F12; Life Technologies, New York, NY) medium supplemented with 15% of fetal bovine serum (FBS - Life Technologies, New York, NY) and antibiotics. For qRT-PCR analysis subconfluent primary cultures were detached (0.05% trypsin-0.53 mM EDTA

- Life Technologies, New York, NY) and subcultured (p=1) at a density 0.2×10^6 cells in 6-well plates (collagen IV coated; Becton Dickinson Labware) in DMEM/F12 medium supplemented with 5% FBS. At 80–90% cell confluency fresh media was added (DMEM/F12 plus 5% FBS) and after 24h of incubation dermal fibroblasts were collected with Trizol for total RNA extraction.

4.9. In situ zymography with quenched fluorogenic DQ-gelatin and DQ-collagen

Subconfluent primary cultures were detached and sub-cultured (p=1) at a density of 0.2×10^6 cells in 35mm glass bottom microwell dishes (MatTek Corporation, Ashland, MA) in DMEM/F12 with 15% FBS. Dermal fibroblasts at 50–60% confluency were washed with DMEM/F12 media without FBS and then incubated over night with DQ gelatin (100μg/ml; Molecular Probes, Eugene, OR) or DQ collagen IV (100μg/ml; Molecular Probes, Eugene, OR) in DMEM/F12 media (no FBS). For the inhibitory assay, selected cultures were pretreated with GM6001 (Chemicon International, Temecula, CA) for 1h. The following day, media were removed and cells were covered with ProLong Gold with DAPI (Molecular Probes, Eugene, OR.). MMPs activity was localized and photographed by Zeiss Meta 510 confocal microscope.

4.10. Statistical analysis

Hydroxyproline, quantitative RT-PCR and densitometric data were analyzed using GraphPad Prism, version 5.0 (GraphPad Software Inc, San Diego, CA). The means and SEM were calculated for each data set. A one-way analysis of variance (ANOVA) with Tukey's post test was used. Statistical significance was set at a p value <0.05.

Acknowledgments

The author thanks Leslie P. Kozak for advice during the course of the work and critical reading of the manuscript and Jessica A. Manuel for excellent technical work. This study was supported by National Institutes of Health; Grant 346 No. RO1 1 P20 RR021945 COBRE and by European Community's Seventh Framework Programme REGPOT – 2010-1; Grant No. 264103 REFRESH. Histological photographs, immuhistochemical detection of MMP-13 expression and immunofluorescent detection of MMPs activity were performed at Cell Biology and Imaging Core, Pennington Biomedical Research Center.

References

Ashcroft GS, Horan MA, Ferguson MW. Aging is associated with reduced deposition of specific extracellular matrix components, an upregulation of angiogenesis, and an altered inflammatory response in a murine incisional wound healing model. J Invest Dermatol. 1997a; 108:430–7. [PubMed: 9077470]

Ashcroft GS, Horan MA, Herrick SE, Tarnuzzer RW, Schultz GS, Ferguson MW. Age-related differences in the temporal and spatial regulation of matrix metalloproteinases (MMPs) in normal skin and acute cutaneous wounds of healthy humans. Cell Tissue Res. 1997b; 290:581–91. [PubMed: 9369533]

Ashcroft GS, Mills SJ, Ashworth JJ. Ageing and wound healing. Biogerontology. 2002; 3:337–45. [PubMed: 12510172]

Barrick B, Campbell EJ, Owen CA. Leukocyte proteinases in wound healing: roles in physiologic and pathologic processes. Wound Repair Regen. 1999; 7:410–22. [PubMed: 10633000]

Bryant SV, Endo T, Gardiner DM. Vertebrate limb regeneration and the origin of limb stem cells. Int J Dev Biol. 2002; 46:887–96. [PubMed: 12455626]

Clark LD, Clark RK, Heber-Katz E. A new murine model for mammalian wound repair and regeneration. Clin Immunol Immunopathol. 1998; 88:35–45. [PubMed: 9683548]

Clark, R. The molecular and cellular biology of wound repair. Plenum Press; New York: 1996.

Colwell AS, Longaker MT, Lorenz HP. Mammalian fetal organ regeneration. Adv Biochem Eng Biotechnol. 2005; 93:83–100. [PubMed: 15791945]

Dang C, Ting K, Soo C, Longaker MT, Lorenz HP. Fetal wound healing current perspectives. Clin Plast Surg. 2003a; 30:13–23. [PubMed: 12636212]

Dang CM, Beanes SR, Lee H, Zhang X, Soo C, Ting K. Scarless fetal wounds are associated with an increased matrix metalloproteinase-to-tissue-derived inhibitor of metalloproteinase ratio. Plast Reconstr Surg. 2003b; 111:2273–85. [PubMed: 12794470]

Ferguson MW, O'Kane S. Scar-free healing: from embryonic mechanisms to adult therapeutic intervention. Philos Trans R Soc Lond B Biol Sci. 2004; 359:839–50. [PubMed: 15293811]

Fujiwara M, Muragaki Y, Ooshima A. Keloid-derived fibroblasts show increased secretion of factors involved in collagen turnover and depend on matrix metalloproteinase for migration. Br J Dermatol. 2005; 153:295–300. [PubMed: 16086739]

Gawronska-Kozak B. Regeneration in the ears of immunodeficient mice: identification and lineage analysis of mesenchymal stem cells. Tissue Eng. 2004; 10:1251–65. [PubMed: 15363180]

Gawronska-Kozak B, Bogacki M, Rim JS, Monroe WT, Manuel JA. Scarless skin repair in immunodeficient mice. Wound Repair Regen. 2006; 14:265–276. [PubMed: 16808805]

Gill SE, Parks WC. Metalloproteinases and their inhibitors: regulators of wound healing. Int J Biochem Cell Biol. 2008; 40:1334–47. [PubMed: 18083622]

Gurtner GC, Werner S, Barrandon Y, Longaker MT. Wound repair and regeneration. Nature. 2008; 453:314–21. [PubMed: 18480812]

Han M, Yang X, Lee J, Allan CH, Muneoka K. Development and regeneration of the neonatal digit tip in mice. Dev Biol. 2008; 315:125–35. [PubMed: 18234177]

Han YP, Tuan TL, Hughes M, Wu H, Garner WL. Transforming growth factor-beta - and tumor necrosis factor-alpha -mediated induction and proteolytic activation of MMP-9 in human skin. J Biol Chem. 2001; 276:22341–50. [PubMed: 11297541]

Hartenstein B, Dittrich BT, Stickens D, Heyer B, Vu TH, Teurich S, Schorpp-Kistner M, Werb Z, Angel P. Epidermal development and wound healing in matrix metalloproteinase 13-deficient mice. J Invest Dermatol. 2006; 126:486–96. [PubMed: 16374453]

Hattori N, Mochizuki S, Kishi K, Nakajima T, Takaishi H, D'Armiento J, Okada Y. MMP-13 plays a role in keratinocyte migration, angiogenesis, and contraction in mouse skin wound healing. Am J Pathol. 2009; 175:533–46. [PubMed: 19590036]

Kobayashi T, Hattori S, Shinkai H. Matrix metalloproteinases-2 and -9 are secreted from human fibroblasts. Acta Derm Venereol. 2003; 83:105–7. [PubMed: 12735637]

Kyriakides TR, Wulsin D, Skokos EA, Fleckman P, Pirrone A, Shipley JM, Senior RM, Bornstein P. Mice that lack matrix metalloproteinase-9 display delayed wound healing associated with delayed reepithelization and disordered collagen fibrillogenesis. Matrix Biol. 2009; 28:65–73. [PubMed: 19379668]

Legrand C, Gilles C, Zahm JM, Polette M, Buisson AC, Kaplan H, Birembaut P, Tournier JM. Airway epithelial cell migration dynamics. MMP-9 role in cell-extracellular matrix remodeling. J Cell Biol. 1999; 146:517–29. [PubMed: 10427102]

Longaker MT, Whitby DJ, Adzick NS, Crombleholme TM, Langer JC, Duncan BW, Bradley SM, Stern R, Ferguson MW, Harrison MR. Studies in fetal wound healing, VI. Second and early third trimester fetal wounds demonstrate rapid collagen deposition without scar formation. J Pediatr Surg. 1990; 25:63–8. discussion 68–9. [PubMed: 2299547]

Lorenz HP, Lin RY, Longaker MT, Whitby DJ, Adzick NS. The fetal fibroblast: the effector cell of scarless fetal skin repair. Plast Reconstr Surg. 1995; 96:1251–9. discussion 1260–1. [PubMed: 7480221]

Madlener M, Parks WC, Werner S. Matrix metalloproteinases (MMPs) and their physiological inhibitors (TIMPs) are differentially expressed during excisional skin wound repair. Exp Cell Res. 1998; 242:201–10. [PubMed: 9665817]

Manuel JA, Gawronska-Kozak B. Matrix metalloproteinase 9 (MMP-9) is upregulated during scarless wound healing in athymic nude mice. Matrix Biol. 2006

Martin P. Wound healing--aiming for perfect skin regeneration. Science. 1997; 276:75–81. [PubMed: 9082989]

Mohan R, Chintala SK, Jung JC, Villar WV, McCabe F, Russo LA, Lee Y, McCarthy BE, Wollenberg KR, Jester JV, Wang M, Welgus HG, Shipley JM, Senior RM, Fini ME. Matrix metalloproteinase

gelatinase B (MMP-9) coordinates and effects epithelial regeneration. J Biol Chem. 2002; 277:2065–72. [PubMed: 11689563]

Occleston NL, Laverty HG, O'Kane S, Ferguson MW. Prevention and reduction of scarring in the skin by Transforming Growth Factor beta 3 (TGFbeta3): from laboratory discovery to clinical pharmaceutical. J Biomater Sci Polym Ed. 2008a; 19:1047–63. [PubMed: 18644230]

Occleston NL, O'Kane S, Goldspink N, Ferguson MW. New therapeutics for the prevention and reduction of scarring. Drug Discov Today. 2008b; 13:973–81. [PubMed: 18824245]

Owen CA, Hu Z, Barrick B, Shapiro SD. Inducible expression of tissue inhibitor of metalloproteinases-resistant matrix metalloproteinase-9 on the cell surface of neutrophils. Am J Respir Cell Mol Biol. 2003; 29:283–94. [PubMed: 12663332]

Page-McCaw A, Ewald AJ, Werb Z. Matrix metalloproteinases and the regulation of tissue remodelling. Nat Rev Mol Cell Biol. 2007; 8:221–33. [PubMed: 17318226]

Park IS, Kim WS. Modulation of gelatinase activity correlates with the dedifferentiation profile of regenerating salamander limbs. Mol Cells. 1999; 9:119–26. [PubMed: 10340464]

Parks WC. Matrix metalloproteinases in repair. Wound Repair Regen. 1999; 7:423–32. [PubMed: 10633001]

Peled ZM, Phelps ED, Updike DL, Chang J, Krummel TM, Howard EW, Longaker MT. Matrix metalloproteinases and the ontogeny of scarless repair: the other side of the wound healing balance. Plast Reconstr Surg. 2002; 110:801–11. [PubMed: 12172142]

Ravanti L, Hakkinen L, Larjava H, Saarialho-Kere U, Foschi M, Han J, Kahari VM. Transforming growth factor-beta induces collagenase-3 expression by human gingival fibroblasts via p38 mitogen-activated protein kinase. J Biol Chem. 1999; 274:37292–300. [PubMed: 10601295]

Ravanti L, Toriseva M, Penttinen R, Crombleholme T, Foschi M, Han J, Kahari VM. Expression of human collagenase-3 (MMP-13) by fetal skin fibroblasts is induced by transforming growth factor beta via p38 mitogen-activated protein kinase. Faseb J. 2001; 15:1098–100. [PubMed: 11292680]

Redd MJ, Cooper L, Wood W, Stramer B, Martin P. Wound healing and inflammation: embryos reveal the way to perfect repair. Philos Trans R Soc Lond B Biol Sci. 2004; 359:777–84. [PubMed: 15293805]

Soo C, Shaw WW, Zhang X, Longaker MT, Howard EW, Ting K. Differential expression of matrix metalloproteinases and their tissue-derived inhibitors in cutaneous wound repair. Plast Reconstr Surg. 2000; 105:638–47. [PubMed: 10697171]

Steffensen B, Hakkinen L, Larjava H. Proteolytic events of wound-healing--coordinated interactions among matrix metalloproteinases (MMPs), integrins, and extracellular matrix molecules. Crit Rev Oral Biol Med. 2001; 12:373–98. [PubMed: 12002821]

Szpaderska AM, Zuckerman JD, DiPietro LA. Differential injury responses in oral mucosal and cutaneous wounds. J Dent Res. 2003; 82:621–6. [PubMed: 12885847]

Toriseva M, Kahari VM. Proteinases in cutaneous wound healing. Cell Mol Life Sci. 2009; 66:203–24. [PubMed: 18810321]

Toriseva MJ, Ala-aho R, Karvinen J, Baker AH, Marjomaki VS, Heino J, Kahari VM. Collagenase-3 (MMP-13) enhances remodeling of three-dimensional collagen and promotes survival of human skin fibroblasts. J Invest Dermatol. 2007; 127:49–59. [PubMed: 16917496]

Vaalamo M, Leivo T, Saarialho-Kere U. Differential expression of tissue inhibitors of metalloproteinases (TIMP-1, -2, -3, and -4) in normal and aberrant wound healing. Hum Pathol. 1999; 30:795–802. [PubMed: 10414498]

Vinarsky V, Atkinson DL, Stevenson TJ, Keating MT, Odelberg SJ. Normal newt limb regeneration requires matrix metalloproteinase function. Dev Biol. 2005; 279:86–98. [PubMed: 15708560]

Wu N, Jansen ED, Davidson JM. Comparison of mouse matrix metalloproteinase 13 expression in free-electron laser and scalpel incisions during wound healing. J Invest Dermatol. 2003; 121:926–32. [PubMed: 14632214]

Wysocki AB, Staiano-Coico L, Grinnell F. Wound fluid from chronic leg ulcers contains elevated levels of metalloproteinases MMP-2 and MMP-9. J Invest Dermatol. 1993; 101:64–8. [PubMed: 8392530]

Yang EV, Gardiner DM, Carlson MR, Nugas CA, Bryant SV. Expression of Mmp-9 and related matrix metalloproteinase genes during axolotl limb regeneration. Dev Dyn. 1999; 216:2–9. [PubMed: 10474160]

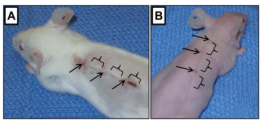

Figure 1.

Macroscopic appearance of skin tissues at post-wounded Day 7 in wild-type, BALB/c (A) and nude, Hsd: Athymic Nude-Foxn1nu (B) mice. Mice were given a 3–4 cm full-thickness dorsal wound that was closed with three stainless steel wound clips which were removed 5 days after wounding. Arrows point out clips locations, brackets indicate skin tissues collected for the analyses.

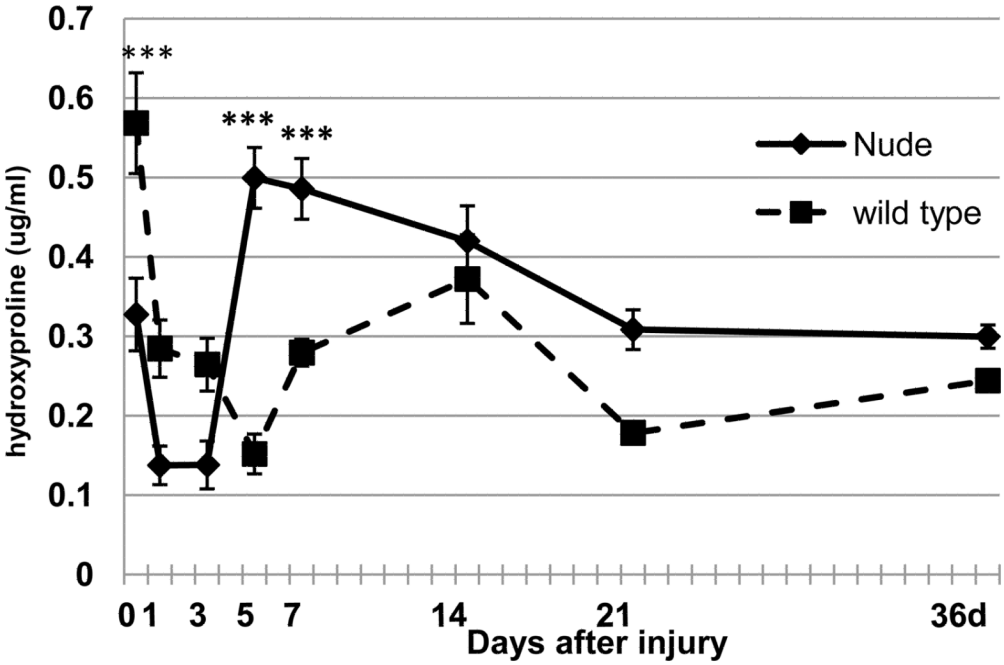

Figure 2.

Collagen levels measured as hydroxyproline content in un-injured (Day 0) and post-injured skin tissues in nude (Hsd: Athymic Nude-Foxn1nu) and wild-type (BALB/c) mice. Data represents the mean ± SEM (n=7–9 per time point). Asterisks indicate significant differences between nude and wild-type mice (***$p<0.001$).

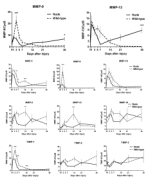

Figure 3.
Quantitative RT-PCR determination of *Mmps* and *Timps* mRNA levels analyzed in nude (Hsd: Athymic Nude-Foxn1nu) and wild-type (BALB/c) mice during the course of skin wound healing process. Expression of *Mmps* and *Timps* mRNA analysed in single skin samples (n=7–9) was normalized by level of cyclophilin B mRNA in the reaction. There are no statistically significant differences in the relative expression of cyclophilin B between nude and wild type mice. Values are the mean ± SEM (n=7–9). Asterisks indicate significant differences between nude and wild-type mice (*p<0.05; **p<0.01; ***p<0.001).

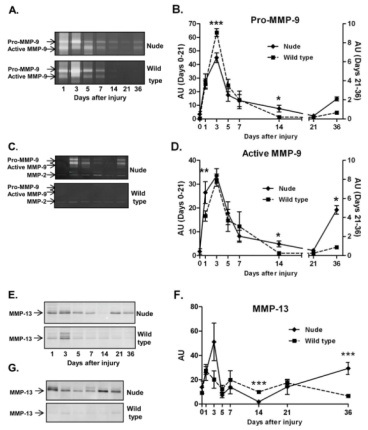

Figure 4.

MMP-9 (A, B, C and D) and MMP-13 (E, F and G) protein expression analysis during the skin wound healing process in (Hsd: Athymic Nude-Foxn1nu) and wild-type (BALB/c) mice. (A) Representative zymographs of MMP-9 expression/activity in individual mice between Day 1 and 36 after injury. (B and D) Densitometric analysis of n=130 animals in 16 zymographs for pro- and active-form of MMP-9 expression/acitvity. (C) Comparison of MMP-9 expression/activity at post-wounded Day 36 of individual skin samples from nude (n=6) and wild type (n=6) mice. (E) Representative Western Blots of MMP-13 expression. (F) Protein levels for MMP-13 were determined by densitometry of 16 Western blots (n=130 animals) in which proteins were detected with Odyssey LI-COR imaging system. (G) Comparison of MMP-13 expression at post-wounded Day 36 based on individual skin samples from nude (n=6) and wild type (n=6) mice. Arrows depict bands for pro- and active-forms of MMP-9 (A and C), MMP-2 (C) and protein for MMP-13 (E and G). Data in B, D and F are represented as the mean ± SEM. Asterisks indicate significant differences between nude and wild-type mice (*p<0.05; **p<0.01; ***p<0.001).

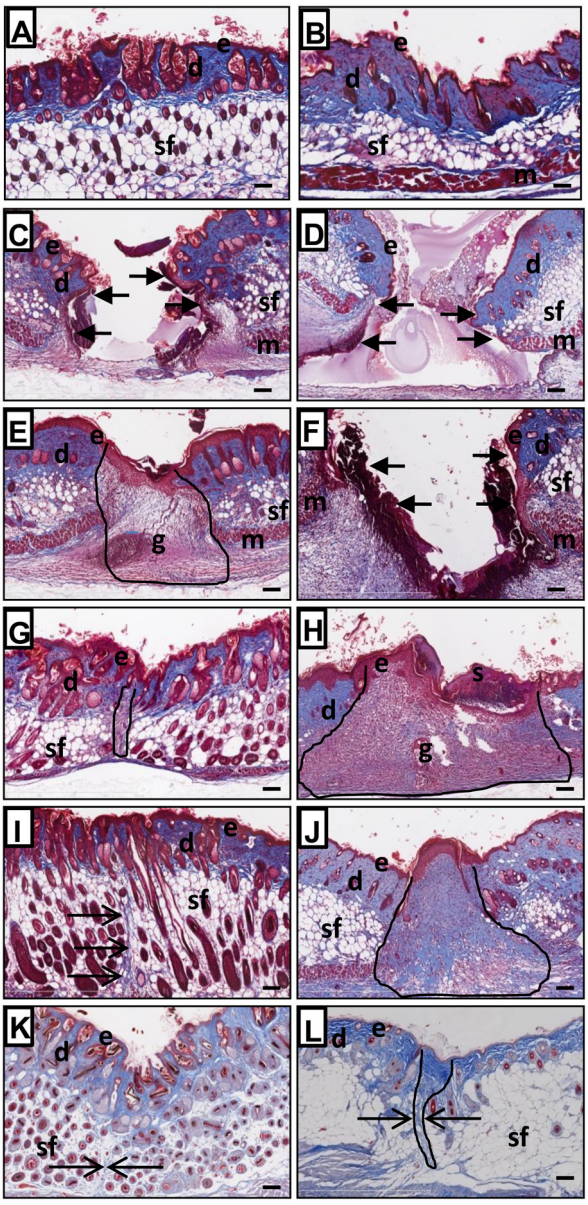

Figure 5.

Masson's trichrome stained skin sections from Hsd: Athymic Nude-Foxn1nu (A, C, E, G, I and K) and BALB/c - wild type (B, D, F, H, J and L) mice collected at post-wounded Day 0 (A and B), Day 1 (C and D), Day 3 (E and F), Day 7 (G and H), Day 14 (I and J) and Day 36 (K and L). Arrows indicate the margins of opened/unhealed wound edges on C, D and F. The post-wounded area are outlined on E, G, H, J and L. Open arrows indicate collagen fibers (blue) on I K and L. Abbreviations: e, epidermis; d, dermis; sf, subcutaneous fat; m, muscle; g, granulation tissue; s, scab. Scale bars: 100μm.

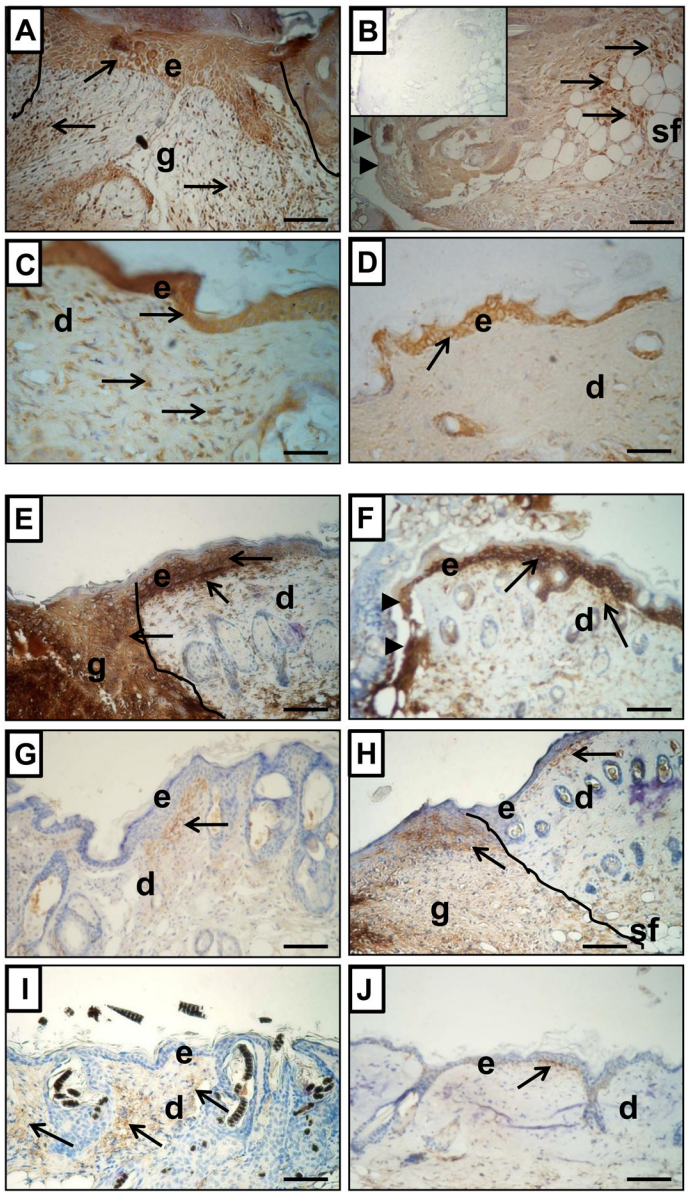

Figure 6.

Immunohistological detection of MMP-9 (A–D) and MMP-13 (E–J) expression in skin samples from Hsd: Athymic Nude-Foxn1nu (A, C, E, G and I) and wild-type BALB/c (B, D, F, H and J) mice at post-wounded Day 3 (A, B, E and F), Day 7 (G–H) and Day 36 (C–D and I–J). The post-wounded area is outlined on A, E and H. Arrowheads indicate the margins of opened/unhealed wound edges on B and F. Arrows indicate MMP-9 or MMP-13 positivity (brown deposits). Sections were counterstained with hematoxylin. Abbreviations: e, epidermis; d, dermis; sf, subcutaneous fat; g, granulation tissue. Insert in B shows control of immunoreaction where first antibody were replaced by non-specific IgG. Scale Bars: 100μm.

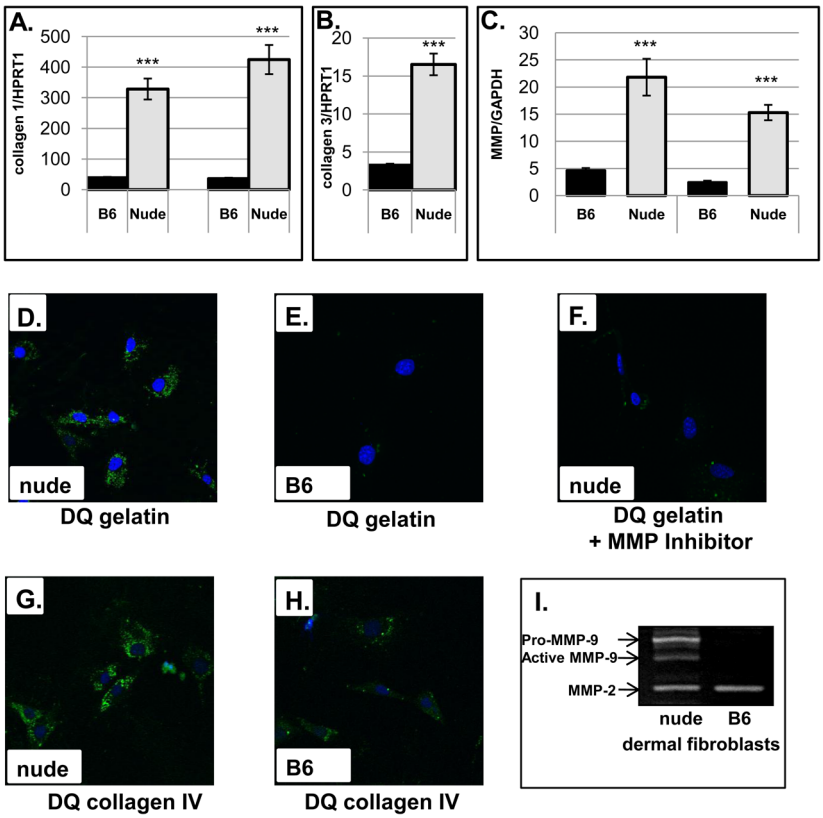

Figure 7.

In vitro analysis of collagen and MMPs expression in cultured nude (Hsd: Athymic Nude-Foxn1nu) and B6 dermal fibroblasts. Collagen I (A), collagen III (B), MMP-9 and MMP-13 (C) mRNA expression was analyzed by quantitative RT-PCR and were normalized to HPRT1 (A and B) and GAPDH (C) expression as an internal control. Data are represented as the mean ± SEM for (A) n=3, (B) n=3 and (C) n=6 separate experiments; ***$p<0.001$. In situ zymography of dermal fibroblasts from nude (D, F and G) and B6 (E and H) mice was analyzed by confocal microscopy. The cells were overlaid with DQ gelatin (D, E and F) or DQ collagen IV (G and H) and incubated for 24 hours. Nude dermal fibroblasts in F were pretreated with nonspecific MMP blocker (GM6001) for 1hour before DQ gelatin treatment. Green staining indicates MMPs digested gelatin or collagen IV whereas blue indicates nuclear staining (DAPI). (I) gelatin zymography. 20 μg of non-denatured protein per sample was run on a 10% electrophoresis gel incorporated with gelatin (1mg/ml). Clear protein lysis bands on a blue background were visualized by staining with Coomassie Blue (Bio-Rad).

Table 1

Expression of *Mmp-2,-3,-8,-9,-10,-12,-13,-14* and *Timp-1, -2, -3* mRNA in non-injured skin tissues from nude (Hsd: Athymic Nude-*Foxn1*^{nu}) and wild type (BALB/c) mice.

	MMP-2	MMP-3	MMP-8	MMP-9	MMP-10	MMP-12*	MMP-13*	MMP-14	TIMP-1	TIMP-2	TIMP-3
nude	5.69±1.8	1.79±0.3	0.11±0.1	2.95±0.7	0.58±0.2	9.73±3.6	2.77±0.8	10.7±4.7	0.78±0.2	7.55±2.4	18.77±5.7
wild type	6.15±0.9	1.65±0.3	0.02±0.01	1.88±0.4	0.15±0.07	1.63±1.05	0.60±0.39	8.5±1.24	0.35±0.07	10.88±2.08	38.92±9.9

Expression *of Mmps* and *Timps* mRNA analysed in single skin samples (n=7–9) was normalized by level of cyclophilin B mRNA in the reaction using standard curve method. There were no statistically significant differences in the cyclophilin B mRNA copy numbers between nude and wild type mice. Values are the mean ± SEM (n=7–9);

* $p<0.05$.

Matrix Biol. Author manuscript; available in PMC 2012 May 1.